

Assessing the Instantaneous Risk of Direct Laser Impingement

Salvatore Alfano*

The Aerospace Corporation, Colorado Springs, Colorado 80910

Several methods are presented for assessing the instantaneous risk of direct laser impingement given uncertainties in object and emitter positions. These methods are constructed to identify those occurrences when the probability of laser impingement exceeds a user-defined threshold. These formulations enhance computational efficiency through use of analytically determined scale factors.

Nomenclature

| | |
|-------------|---|
| $A(K)$ | = area of scaled ellipse |
| $A2'$ | = projected primary object position (two dimensional) |
| $A3$ | = primary object position (three dimensional) |
| $B2$ | = position of combined object from ellipse center (two dimensional) |
| $B2'$ | = projected secondary object position (two dimensional) |
| $B3$ | = secondary object position (three dimensional) |
| $C2$ | = scaled and combined covariance matrix (two dimensional) |
| $CA2$ | = projected primary object position covariance (two dimensional) |
| $CA3$ | = primary object position covariance (three dimensional) |
| $CB2$ | = projected secondary object position covariance (two dimensional) |
| $CB3$ | = secondary object position covariance (three dimensional) |
| $CL2$ | = projected laser emitter position covariance (two dimensional) |
| $CL3$ | = laser emitter position covariance (three dimensional) |
| DA | = distance from emitter to primary object |
| DB | = distance from emitter to secondary object |
| K | = ellipse scale factor |
| K_{HI} | = ellipse scale factor upper bound |
| K_{LO} | = ellipse scale factor lower bound |
| $L2$ | = laser emitter position projected into prime system (two dimensional) |
| $L3$ | = laser emitter position (three dimensional) |
| $LOS3$ | = line-of-sight vector from emitter to primary object (three dimensional) |
| M | = alternate representation of ellipse scale factor |
| OBJ | = combined object radius |
| P | = probability of laser impingement |
| \tilde{P} | = estimate of probability of laser impingement |
| q | = intermediate value |
| $R3$ | = rotation matrix |
| r | = intermediate value |

| | |
|------------------------------------|-----------------------------|
| S | = intermediate matrix |
| T | = translation matrix |
| $\alpha 0M, \alpha 11, \alpha 1M,$ | = intermediate coefficients |
| $\alpha 21, \alpha 2M$ | |
| λ | = eigenvalue |

Introduction

PREDICTIVE avoidance analysis for laser emissions should reasonably ensure that neighboring objects are not inadvertently illuminated. Typically, one determines whether and when a secondary object will transgress a user-defined circular safety cone.^{1,2} The cone axis is along the line-of-sight vector as measured from the laser beam source to the primary object with its half-angle based on estimates of positional accuracy (Fig. 1). For space objects, prescreening of neighboring satellites can greatly reduce the computational burden.^{1†} Predictive analysis should assess the risk of satellite-to-satellite and satellite-to-ground communication interference. For high-energy lasers, it is imperative to balance mission objectives against possible degradation or disruption of neighboring objects.

If the uncertainties associated with emitter location and object position can be represented by three-dimensional Gaussian probability densities, then the probability of direct laser impingement on a secondary object can be calculated. These densities take the form of covariance matrices and can be obtained from the owner-operators or independent surveillance sources such as the U.S. Satellite Catalog (Special Perturbations). Because the probability calculations can be computationally burdensome, it is always desirable to prescreen candidate objects.¹ The traditional safety-cone approach can be overly conservative if the shape is not tailored to the probability density. Such cones are circular and larger than necessary, scaled to the size of the axis of greatest uncertainty. As has been verified with launch collision avoidance, such conservatism can deny opportunities that have very low incidental probabilities.³ Objects that are predicted to enter such cones should be further evaluated so as not to unnecessarily hinder operations.

The methods described here can be used to assess the instantaneous risk of direct laser impingement on a secondary object. Covariances of emitter and object locations are scaled, projected into a plane perpendicular to the beam, and then combined. Object and beam sizes, represented as circles in the plane, are also combined and then translated to the mean location of the secondary in the plane. An analytical method is introduced to determine the covariance scale factors such that the combined object circle is just touched by the resulting covariance ellipse on the near and far sides. The near-scale factor can be used as a decision threshold for closing the lasing window. If further analysis is desired, the near- and far-scale factors can be used to set the limits of integration to rigorously determine probability. These same scale factors can be used to estimate the probability without integration by analyzing a simple ratio.

Received 12 March 2002; revision received 10 October 2002; accepted for publication 4 February 2003. Copyright © 2003 by Salvatore Alfano. Published by the American Institute of Aeronautics and Astronautics, Inc., with permission. Copies of this paper may be made for personal or internal use, on condition that the copier pay the \$10.00 per-copy fee to the Copyright Clearance Center, Inc., 222 Rosewood Drive, Danvers, MA 01923; include the code 0022-4650/03 \$10.00 in correspondence with the CCC.

*Senior Project Engineer, 1150 Academy Park Loop, Suite 136. Associate Fellow AIAA.

†http://www.stk.com/products/explore/products/cat_prod_desc.cfm [cited 6 October 2001].

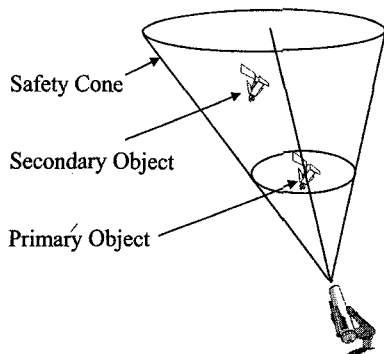


Fig. 1 Safety cone centered on primary object.

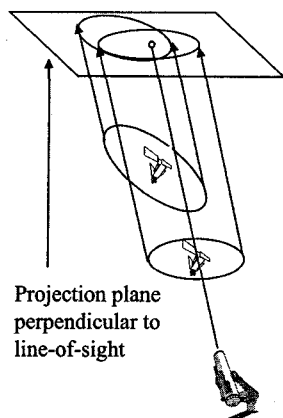


Fig. 2 Object and covariance projections onto the plane.

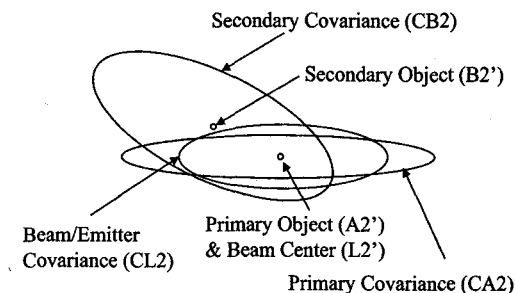


Fig. 3 Projections in the plane.

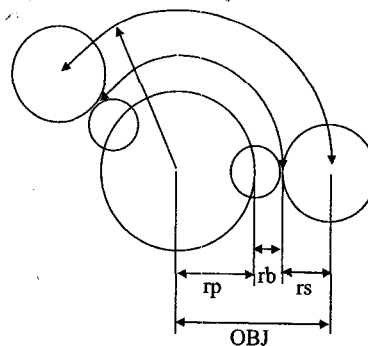
Coordinate Reduction Through Projection

Although two ellipsoids may not share the same space, when viewed from certain angles one may appear to cover or overlap the other (Fig. 2). Analysis of such circumstances is necessary to prevent accidental laser illumination if a secondary object is in or near the line of sight of the primary. Let $L3$ be the three-element Cartesian vector representing mean laser emitter position with the associated 3×3 covariance matrix $CL3$. In a similar manner, let $A3$ and $B3$ be the respective positions of the primary and secondary objects with covariance matrices $CA3$ and $CB3$. The line-of-sight vector $LOS3$ from emitter to primary object is computed as

$$LOS3 = A3 - L3 \quad (1)$$

DA is defined as the magnitude of the $LOS3$ vector. This formulation can be altered to account for the laser searching to acquire the primary object by replacing $LOS3$ with the pointing vector. To simplify calculations, a new coordinate system centered at the emitter is defined using the unitized line-of-sight vector as the z' axis. The x' and y' axes should be chosen to form an orthonormal system. An appropriate rotation matrix $R3$ is then found to transform all vectors and matrices to the prime system.

Once in the prime system, projection to the plane perpendicular to the beam is done by eliminating the z' components. In this two-dimensional space, the projected data are represented as $L2'$, $CL2$, $A2'$, $CA2$, $B2'$, and $CB2$ (Fig. 3), where the previously described



Radii of primary (rp), secondary (rs), and beam (rb)

Fig. 4 Combining radii to form OBJ radius on the projection plane.

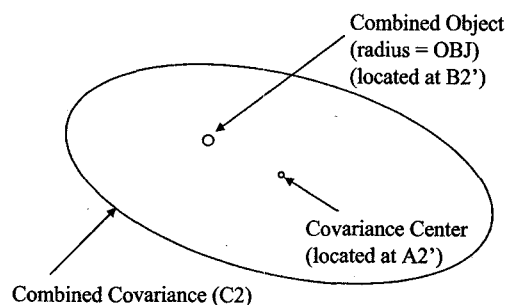


Fig. 5 Combined projection in the plane.

three-dimensional naming convention is preserved but reduced to two in the prime frame. Although the method outlined in Refs. 4 and 5 can accommodate any quadric representation, the primary and secondary objects are considered spherical for this analysis such that their projections become circles on the plane. Assuming that the center of the beam is located somewhere in the primary circle (laser on target), the primary's projected radius (rp) is added to the secondary's (rs) to form the combined object radius OBJ (Fig. 4). If known, the radius of beam spread at the distance DB should also be summed in the OBJ computation. The combined object is centered at $B2'$. Figure 1 shows the relationships that form the OBJ radius. As previously mentioned, this formulation can be altered to account for laser search (and associated pointing uncertainty) prior to acquisition by letting OBJ be the sum of beam and secondary object radii or some arbitrarily defined large value that accommodates the search space and making $LOS3$ the boresight vector.

The covariance matrices are assumed uncorrelated so that, as part of the projection process, they can be scaled and summed to produce the overall covariance matrix $C2$ as explained by Chan⁶:

$$C2 = CL2 \cdot \left(\frac{DB - DA}{DA} \right)^2 + CA2 \cdot \left(\frac{DB}{DA} \right)^2 + CB2 \quad (2)$$

The resulting ellipse is centered at $A2'$ (Fig. 5). For convenience, the coordinate center is translated to $A2'$ and $B2$ is defined as the displacement of the combined object from ellipse center:

$$B2 = B2' - A2' \quad (3)$$

Determining Covariance Scale Factors

The analytical method to determine when ellipses overlap^{4,7} is used here to determine what scale factors cause the covariance $C2$ to just touch the combined object circle on the near and far sides. The method involves adding an extra dimension to the solution space and examining eigenvalues that are associated with degenerate quadric surfaces. To be consistent with covariance matrix inversion, a factor M is introduced as the square of the inverse of the ellipse scale factor K ($M = K^{-2}$). The eigenvalue equation is formed from the

translation matrix T and the intermediate matrix S as

$$T = \begin{bmatrix} 1 & 0 & 0 \\ 0 & 1 & 0 \\ -B2_0 & -B2_1 & 1 \end{bmatrix} \quad (4)$$

$$S = \begin{bmatrix} \lambda & 0 & 0 \\ 0 & \lambda & 0 \\ 0 & 0 & \lambda \end{bmatrix} - \begin{bmatrix} C2_{0,0} & C2_{0,1} & 0 \\ C2_{0,1} & C2_{1,1} & 0 \\ 0 & 0 & -M \end{bmatrix} \cdot T \cdot \begin{bmatrix} 1 & 0 & 0 \\ 0 & 1 & 0 \\ 0 & 0 & -OBJ^2 \end{bmatrix} T^T \quad (5)$$

$$|S| = \lambda^3 + (\alpha 2M \cdot M + \alpha 21) \cdot \lambda^2 + (\alpha 1M \cdot M + \alpha 11) \cdot \lambda + \alpha 0M \cdot M \quad (6)$$

where all arrays are zero-indexed (numbering starts with zero) and

$$\alpha 2M = (B2_1)^2 - OBJ^2 + (B2_0)^2 \quad (7)$$

$$\alpha 21 = -C2_{1,1} - C2_{0,0} \quad (8)$$

$$\alpha 1M = (C2_{0,0} + C2_{1,1}) \cdot OBJ^2 - C2_{0,0} \cdot (B2_1)^2 - C2_{1,1} \cdot (B2_0)^2 + 2 \cdot B2_1 \cdot C2_{0,1} \cdot B2_0 \quad (9)$$

$$\alpha 11 = C2_{0,0} \cdot C2_{1,1} - (C2_{0,1})^2 \quad (10)$$

$$\alpha 0M = [-C2_{0,0} \cdot C2_{1,1} + (C2_{0,1})^2] \cdot OBJ^2 \quad (11)$$

The determinant of S is dependent on M . The values of M must be found such that the $C2$ ellipse just touches the near and far sides of the combined object. Knowing that these conditions occur only when there are two real, identical eigenvalues, the cubic discriminant⁷ is used to solve for M with intermediate values q and r :

$$q = (\alpha 1M \cdot M + \alpha 11)/3 - [(\alpha 2M \cdot M + \alpha 21)^2]/9 \quad (12)$$

$$r = [(\alpha 1M \cdot M + \alpha 11) \cdot (\alpha 2M \cdot M + \alpha 21) - 3 \cdot \alpha 0M \cdot M]/6 - [(\alpha 2M \cdot M + \alpha 21)^3]/27 \quad (13)$$

$$0 = q^3 + r^2 \quad (14)$$

This equation becomes fourth order in M ; its solution yields the minimum and maximum real values of M and, subsequently, the far- and near-scale factors K_{HI} and K_{LO} . It is possible for the combined object circle to envelop the origin; in this case the lower scale factor K_{LO} is set to an arbitrarily small positive number.

K_{LO} represents the size of an elliptically shaped covariance cone that is properly scaled to just touch the combined object in the projected plane. As an example, if K_{LO} is equal to three, then the closest point of the combined object is three sigma from the center in two-dimensional space. The probability of being inside a three-sigma ellipse is 98.9%. The combined object circle occupies only a small space outside the K_{LO} boundary, guaranteeing that the instantaneous probability of laser impingement is significantly less than 1.1%. If desired, K_{LO} can be used by itself to determine window closure based on entering a safety cone that is now optimally shaped by the combined Gaussian probability density.

Probability and Its Estimate

The values of $C2$, $B2$, and OBJ contain all of the information to precisely determine the instantaneous probability P of laser impingement:

$$P = \int_{B2_0 - OBJ}^{B2_0 + OBJ} \int_{B2_1 - \sqrt{OBJ^2 - (x - B2_0)^2}}^{B2_1 + \sqrt{OBJ^2 - (x - B2_0)^2}} \exp \left\{ \frac{-1}{2} \cdot \left[(x \ y) \cdot C2^{-1} \cdot \begin{pmatrix} x \\ y \end{pmatrix} \right] \right\} dy dx \left/ \left[2 \cdot \pi \cdot \sqrt{C2_{0,0} C2_{1,1} - (C2_{0,1})^2} \right] \right. \quad (15)$$

This equation can be reduced to a single integral using error functions, but its computation can still be burdensome. An alternate form of reduction can be found in the work of Patena.⁸

An algebraic approximation may be suitable for those conditions where the combined object radius is smaller than the covariance ellipse's minor axis and does not envelop the ellipse's center. The probability of being anywhere inside the ellipse is solely determined from the scale factor K as

$$P(K) = 1 - \exp(-1/2 \cdot K^2) \quad (16)$$

The area of the scaled ellipse is simply

$$A(K) = K^2 \cdot \pi \cdot \sqrt{C2_{0,0} C2_{1,1} - (C2_{0,1})^2} \quad (17)$$

and the area of the combined object is

$$A_{OBJ} = \pi \cdot OBJ^2 \quad (18)$$

An estimate for P can be made by assuming that probability directly corresponds to area in the vicinity of the combined object. This estimate manifests itself as a ratio leading to the approximation

$$\tilde{P} = \frac{P(K_{HI}) - P(K_{LO})}{A(K_{HI}) - A(K_{LO})} \cdot A_{OBJ} \quad (19)$$

Making the appropriate substitutions yields the algebraic expression

$$\tilde{P} = \frac{[-\exp(-1/2 \cdot K_{HI}^2) + \exp(-1/2 \cdot K_{LO}^2)] \cdot (OBJ)^2}{(K_{HI}^2 - K_{LO}^2) \cdot \sqrt{C2_{0,0} C2_{1,1} - (C2_{0,1})^2}} \quad (20)$$

The reader is reminded that this is only an estimate whose accuracy is related to OBJ distance from the center and its size relative to the covariance. The conditions for using this approximation should be carefully crafted to ensure that its accuracy is always within decision-making bounds. Numerical evaluation has shown that if K_{LO} is greater than zero and OBJ is less than one-ninth of the semiminor axis of the ellipse formed by $C2$, then for probabilities greater than 10^{-10} the estimate will always be within 1% of actual.

Results

A test case was chosen based on the one presented in Ref. 1 to compare and contrast window closures based on probability and safety cones. The target satellite was MIR (catalog number 16609) with all its modules included. Combining KVANT 1, KVANT 2, KRYSTALL, SPEKTR, SOYUZ TM, and the core module yielded a total radar cross section of 1574 m². No consideration was given to attitude as the object was treated as a sphere for this analysis. The lasing platform was located at 104°W longitude and 35°N latitude, with an elevation of 1935.5 m and uncertainty of 10 m (one sigma) in all directions; the laser beam was considered to have a half-angle divergence of 0.25 mrad. The test case began 28 Sept. 1995 at 16:07 Greenwich mean time (GMT) and ended 4 min later. Publicly available NORAD two-line element sets were used to determine satellite positions; associated radar cross sections and three-sigma variances are listed in Table 1. The primary variance axis is along the velocity vector, the tertiary axis is along the momentum vector, and the secondary axis completes the right-hand system (nadir pointing for circular orbits).

The safety cone half-angle was narrowed from the original 5 deg presented in Ref. 1. Half-angles of 2 and 1 deg were chosen for this analysis, with all objects passing within the safety cones listed in Table 2. The 2-deg analysis produced a total closure of 1.14 min in the 4-min window, whereas the 1-deg analysis produced 0.41 min of closure. The risk analysis produces a window closure of only

Table 1 Satellite radar cross sections and variances

| Satellite identification number | Cross section, m ² | 3 σ (along V), km | 3 σ (~nadir), km | 3 σ (normal), km |
|---------------------------------|-------------------------------|--------------------------|-------------------------|-------------------------|
| 3431 | 1.9688 | 21.69 | 5.96 | 14.07 |
| 7003 | 2.9243 | 6.11 | 0.86 | 1.54 |
| 9862 | 5.6864 | 21.69 | 5.96 | 14.07 |
| 10949 | 6.4262 | 33.70 | 9.20 | 22.22 |
| 12472 | 3.1477 | 21.69 | 5.96 | 14.07 |
| 12855 | 259.8169 | 21.69 | 5.96 | 14.07 |
| 13012 | 18.394 | 33.60 | 9.17 | 22.15 |
| 15098 | 5.4204 | 34.45 | 9.54 | 22.64 |
| 16925 | 7.3418 | 34.45 | 9.54 | 22.64 |
| 18578 | 3.2522 | 21.26 | 5.80 | 14.01 |
| 19215 | 3.2804 | 15.82 | 4.32 | 10.43 |
| 19776 | 2.6387 | 15.82 | 4.32 | 10.43 |
| 20433 | 10.7579 | 5.66 | 0.94 | 1.77 |
| 20926 | 3.6488 | 15.82 | 4.32 | 10.43 |
| 21216 | 0.9002 | 13.48 | 11.52 | 5.40 |
| 21941 | 10.9863 | 34.45 | 9.54 | 22.64 |
| 22057 | 1.5598 | 8.32 | 6.68 | 4.35 |
| 22061 | 1.0406 | 5.83 | 4.35 | 4.35 |
| 22176 | 12.9704 | 3.75 | 0.62 | 1.17 |
| 22671 | 9.8704 | 34.45 | 9.54 | 22.64 |
| 22726 | 42.7872 | 6.11 | 0.86 | 1.54 |
| 23452 | 0.6967 | 13.48 | 11.52 | 5.40 |
| 23536 | 12.3897 | 21.69 | 5.96 | 14.07 |

Table 2 Safety cone entry and exit times

| Satellite identification number | 2-deg entry | 2-deg exit | 1-deg entry | 1-deg exit |
|---------------------------------|-------------|------------|-------------|------------|
| 3431 | 3.01 | 3.14 | N/A | N/A |
| 7003 | 2.91 | 3.03 | N/A | N/A |
| 9862 | 2.82 | 2.94 | 2.86 | 2.90 |
| 10949 | 0.33 | 0.51 | N/A | N/A |
| 12472 | 2.85 | 2.92 | N/A | N/A |
| 12855 | 2.88 | 3.01 | 2.92 | 2.97 |
| 13012 | 1.43 | 1.48 | N/A | N/A |
| 15098 | 2.97 | 3.04 | N/A | N/A |
| 16925 | 1.15 | 1.23 | N/A | N/A |
| 18578 | 2.94 | 3.07 | 2.98 | 3.03 |
| 19215 | 3.00 | 3.13 | 3.06 | 3.07 |
| 19776 | 2.95 | 3.03 | N/A | N/A |
| 20433 | 0.91 | 1.00 | 0.94 | 0.97 |
| 20926 | 3.07 | 3.19 | N/A | N/A |
| 21216 | 1.14 | 1.24 | 1.17 | 1.22 |
| 21941 | 3.17 | 3.34 | 3.21 | 3.29 |
| 22057 | 1.09 | 1.17 | N/A | N/A |
| 22061 | 1.11 | 1.22 | 1.15 | 1.19 |
| 22176 | 3.15 | 3.30 | N/A | N/A |
| 22671 | 1.92 | 1.98 | 1.94 | 1.96 |
| 22726 | 3.14 | 3.26 | N/A | N/A |
| 23452 | 3.26 | 3.43 | 3.31 | 3.37 |
| 23536 | 3.21 | 3.31 | N/A | N/A |

0.02 min based on probability exceeding 10^{-9} . Satellite 21216 (GLONASS) closed the window from 1.18 to 1.20 with a maximum probability of 1.24×10^{-8} . For all of the satellites listed, the algebraic probability estimate [Eq. (20)] was always within 1% of the integration [Eq. (15)] and produced the same window closure of 0.02 min.

Effects of Assumptions

Analysis is only as good as the assumptions on which it is based. Greater uncertainty in laser emitter location can cause a dilution of the probability estimate. For such cases it might be prudent to examine the location that yields the greatest probability (i.e., worst-case

scenario). One might assume that the primary object location is perfectly known if it is being illuminated; in that case CA3 should be set to zero. No consideration was given in this work to the screening (shadowing) effect that the primary object might have on the secondary. This formulation can be easily altered to accommodate such occurrences. Models for diffraction, jitter, wave-front error, focus, aperture shape (rectangular vs circular), mode, and intensity pattern can be included to better define the beam size and its covariance.

This work examines the instantaneous risk of laser impingement, whereas some satellites might be more vulnerable to the cumulative effects. Those satellites would require a different analysis, such as the one presented by Patera.⁹ The method just presented deals with laser impingement without consideration of the secondary satellite's tolerance to such. An additional screening could be done to determine whether a given satellite's known or stated threshold would be exceeded.

Conclusions

Several methods are presented for assessing the instantaneous risk of direct laser impingement given uncertainties in object and emitter positions. The primary and secondary objects are modeled as spheres and projected to a plane perpendicular to the laser beam boresight; beam width (divergence) can also be included. Covariances of the objects and emitter location are combined and also projected onto the plane after appropriate scaling. The probability of laser impingement is determined from the relation of combined object area to combined covariance. This probability calculation is done with both mathematical rigor and approximation techniques involving scaled covariance ellipses that just touch the combined object on the near and far sides.

Acknowledgments

Glenn Peterson, a Member of the Technical Staff at The Aerospace Corporation, provided the radar cross sections and variances used in this work. Russ Patera, also a Member of the Technical Staff at The Aerospace Corporation, provided checks of these results using independent tools he developed for Ref. 9.

References

- ¹Alfano, S., Burns, R., Pohlen, D., and Wirsig, G., "Predictive Avoidance for Ground-Based Laser Illumination," *Journal of Spacecraft and Rockets*, Vol. 37, No. 1, 2000, pp. 122-128.
- ²Morris, R. F., and Racca, R. A., "Theater High Energy Laser (THEL) SkyPlot Software Validation," Space Warfare Center, Analysis and Engineering TR 99-12, Colorado Springs, CO, Nov. 1999.
- ³Oltrogge, D., and Gist, R., "Collision Vision Situational Awareness for Safe and Reliable Space Operations," 50th International Astronautical Congress, Paper IAA-99-IAA.6.6.07, Amsterdam, Oct. 1999.
- ⁴Chan, K., "A Simple Mathematical Approach for Determining Intersection of Quadratic Surfaces," American Astronautical Society/AIAA Astrodynamics Specialist Conf., Quebec, AAS Paper 01-358, July-Aug. 2001.
- ⁵Alfano, S., and Greer, M. L., "Determining If Two Ellipsoids Share the Same Volume," American Astronautical Society/AIAA Astrodynamics Specialist Conf., Quebec, AAS Paper 01-357, July-Aug. 2001.
- ⁶Chan, K., "Collision Probability Analyses for Earth Orbiting Satellite," *Advances in the Astronautical Sciences*, Vol. 96, Univelt, San Diego, CA, 1997, pp. 1033-1048.
- ⁷Eshbach, O., and Souders, M., *Handbook of Engineering Fundamentals*, Wiley, New York, 1975, p. 223.
- ⁸Patera, R. P., "General Method for Calculating Satellite Collision Probability," *Journal of Guidance, Control, and Dynamics*, Vol. 24, No. 4, 2001, pp. 716-722.
- ⁹Patera, R. P., "The Probability of a Laser Illuminating a Space Object," American Astronautical Society/AIAA Astrodynamics Specialist Conf., San Antonio, TX, AAS Paper 02-174, Jan. 2002.

D. L. Cooke
Associate Editor